Peer-reviewed version available at Int. J. Mol. Sci. 2019, 20, 3767; doi:10.3390/ijms20153767

Article

Gene expression profiling reveals that PXR activation inhibits hepatic PPARα activity and decreases FGF21 secretion in male C57Bl6/J mice

Sharon Ann Barretto [1,*], Frederic Lasserre [1,*], Anne Fougerat [1], Lorraine Smith [1], Tiffany Fougeray [1], Celine Lukowicz [1], Arnaud Polizzi [1], Sarra Smati [1], Marion Régnier [1], Claire Naylies [1], Colette Bétoulières [1], Yannick Lippi [1], Hervé Guillou [1], Nicolas Loiseau [1], Laurence Gamet-Payrastre [1], Laila Mselli-Lakhal [1] and Sandrine Ellero-Simatos [1,*]

[1] Institut National de la Recherche Agronomique (INRA), UMR1331 Toxalim, Toulouse, France; Sharon.barretto@inra.fr (SAB), Frederic.lasserre@inra.fr (FL), anne.fougerat@inra.fr (AF), lorraine.smith@inra.fr (LS), tiffany.fougeray@inra.fr (TF), celine.lukowicz@inra.fr (CL), arnaud.polizzi@inra.fr (AP), sarra.smati@inra.fr (SS), marion.regnier@inra.fr (MR), claire.naylies@inra.fr (CN), Colette.betoulieres@inra.fr (CB), yannick.lippi@inra.fr (YL), herve.guillou@inra.fr (HG), nicolas.loiseau@inra.fr (NL), Laurence.payrastre@inra.fr (LGP), laila.lakhal@inra.fr (LML)

* Correspondence: sandrine.ellero-simatos@inra.fr

Abstract: The pregnane X receptor (PXR) is the main nuclear receptor regulating the expression of xenobiotic metabolizing enzymes and is highly expressed in the liver and intestine. Recent studies have highlighted its additional role in lipid homeostasis, however, the mechanisms of these regulations are not fully elucidated. We investigated the transcriptomic signature of PXR activation in the liver of adult wild-type vs *Pxr*$^{-/-}$ C57Bl6/J male mice treated with the rodent specific ligand pregnenolone 16α-carbonitrile (PCN). PXR activation increased liver triglyceride accumulation and significantly regulated the expression of 1215 genes mostly xenobiotic metabolizing enzymes. Among the down-regulated genes, we identified a strong peroxisome proliferator-activated receptor α (PPARα) signature. Comparison of this signature with a list of fasting-induced PPARα target genes confirmed that PXR activation decreased the expression of more than 25 PPARα target genes, among which the hepatokine fibroblast growth factor 21 (*Fgf21*). PXR activation abolished plasmatic levels of FGF21. We provide a comprehensive signature of PXR activation in the liver and identify new PXR target genes that might be involved in the steatogenic effect of PXR. Moreover, we show that PXR activation down-regulates hepatic PPARα activity and FGF21 circulation, which could participate in the pleiotropic role of PXR in energy homeostasis.

Keywords: nuclear receptors, hepatokines, transcriptomics

1. Introduction

Peer-reviewed version available at Int. J. Mol. Sci. 2019, 20, 3767; doi:10.3390/ijms20153767

Pregnane X receptor (PXR, systematic name NR1I2) is a member of the nuclear receptor superfamily and is highly expressed in the liver and intestine of mammals [1]. PXR was characterized as a xenosensor that regulates the expression of xenobiotic metabolizing enzymes and transporters, thereby facilitating elimination of xenobiotics and endogenous toxic chemicals such as bile acids [2]. Upon ligand-binding, PXR translocates to the nucleus, heterodimerizes with retinoid X receptor (RXR, NR2B1) and binds to PXR direct repeat 4 (DR-4) response elements (PXRE) that are usually located upstream of target genes. Because of an unusually large and flexible binding pocket, PXR can be activated by a variety of structurally diverse chemicals including pharmaceutical drugs, dietary supplements, herbal medicines, environmental pollutants and endogenous molecules [3]. In line with the role of PXR as a master regulator of xenobiotic metabolism, its first described target gene was cytochrome P450 (CYP) 3A4 in humans [4], which represents 10% of all clinically relevant drug-metabolizing CYPs in the human liver and up to 75-85% in the intestine [5] and is responsible for the metabolization of 60% of marketed drugs [6].

Besides its original function as part of the detoxification machinery, recent studies have also unveiled functions for PXR in intermediary metabolism. There is an increasing amount of clinical evidence showing that PXR agonists cause hyperglycaemia in humans [7] and pre-clinical work suggesting that PXR regulates hepatic glucose metabolism but there is still no solid understanding of the consequences or of the mechanisms involved. Activated PXR has been shown to repress expression of the gluconeogenic genes glucose-6-phosphatase (G6Pase) and phosphoenopyruvate carboxykinase (PEPCK) [8], and of genes involved in glucose uptake such as GLUT2 and of glucokinase (GCK) [9]. Although there is limited data on the relationship between PXR and fatty liver in humans *in vivo*, many studies have demonstrated that PXR activation also causes hepatic lipid accumulation in human cell models and *in vitro* and *in vivo* mouse models [7,10]. This pro-steatotic effect is thought to result from both activation of lipogenesis and inhibition of ß-oxidation [7]. However, the mechanisms by which PXR activation induces perturbations of lipid metabolism are not fully elucidated. Recently, it was shown that activation of intestinal PXR signaling induced dyslipidemia and intestinal cholesterol accumulation [11], while activation of hepatic PXR signaling was sufficient to promote hypercholesterolemia and hepatic lipid accumulation [12].

Here, we aimed to gain insights into the mechanisms of PXR-induced hepatic triglyceride accumulation and performed a transcriptomic comparison of the hepatic gene profiles of WT vs. *Pxr*$^{-/-}$ male mice treated with the rodent specific PXR ligand pregnenolone 16α-carbonitrile (PCN). As expected, we observed that PCN treatment induced hepatic steatosis. We unraveled several previously unknown PXR target genes involved in liver lipid accumulation and discovered a very robust PPARα signature amongst the PXR down-regulated target genes. The PXR-induced decrease in PPARα activity included the regulation of the hepatokine FGF21, a

Peer-reviewed version available at Int. J. Mol. Sci. 2019, 20, 3767; doi:10.3390/ijms20153767

liver-derived hormone with major endocrine roles [13]. This cross-talk between PXR and PPARα in the regulation of FGF21 may contribute to endocrine disruption by xenobiotics acting as ligands for PXR.

2. Results

2.1. Effect of PXR activation on physiological parameters and liver lipids

We investigated the effect of PXR activation by its pharmacological ligand PCN in WT and Pxr-/- male mice. PCN treatment did not affect body weight but increased relative liver mass in a PXR-dependent way. In the liver, PXR activation significantly increased cholesterol esters and triglyceride levels (Figure 1A). In the plasma, PXR activation increased alanine transaminase and decreased total cholesterol levels but did not impact free fatty acids or triglycerides (Figure 1B).

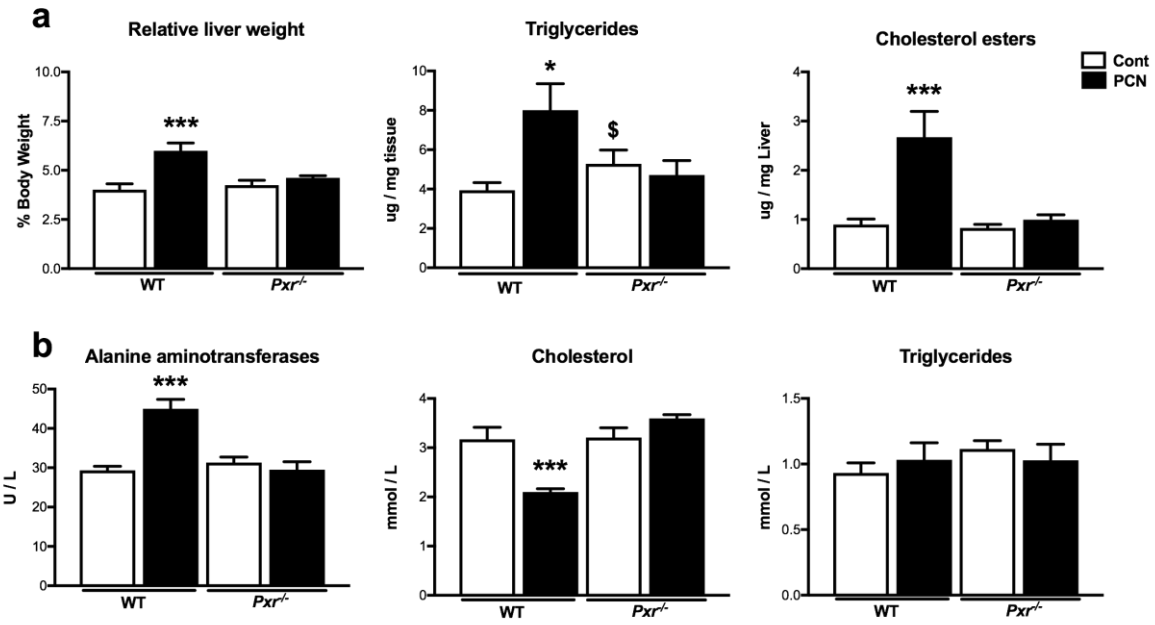

Figure 1. Effect of PCN treatment on liver parameters (a) and plasma biochemistry (b). Data are shown as mean±SEM of n=5-6 per group. *p≤0.05, **p≤0.01, ***p≤0.005 for PCN effect using 2-way ANOVA and Tukey's post-tests. $p≤0.05 for genotype effect.

2.2 Effects of PXR activation on the hepatic transcriptome

Using microarrays, we obtained global transcriptional profiles. Principal component analysis (PCA) first illustrated that PCN treatment significantly impacted the hepatic transcriptome (Figure 2A). The discrimination of WT PCN vs. WT Cont seems stronger than that of the *Pxr*$^{-/-}$ PCN vs. *Pxr*$^{-/-}$ Cont, confirming, as expected, a significant PXR-dependent transcriptional effect of PCN.

We next sought to decipher the biological functions affected by PXR activation. We used linear models and considered genes to be significantly regulated with a fold-change > 1.5 and a FDR < 0.05. PCN treatment significantly up-regulated the expression of 1258 genes in WT animals, and of 333 genes in *Pxr*$^{-/-}$ mice (Figure 2C).

Using the 1029 "prototypical" PXR target genes (those that were up-regulated only in WT animals), we conducted a pathway enrichment analysis, which revealed 7 functional clusters significantly enriched (Figure 2D and Supplementary Table 2) with genes involved in cell cycle, cell division and mitosis, glutathione metabolism, cytochromes P450, lipid metabolism, chemotaxis and positive regulation of inflammatory response. Figure 2E confirms these results by illustrating the fold-changes of the top 30 most upregulated genes. These results first confirmed the well-described influence of PXR activation on hepatic xenobiotic metabolizing enzymes, mainly those from the Cyp3 family. Supplementary Table 3 provides the full description of the impact of PCN treatment on all xenobiotic metabolizing enzymes. Induction of 2 of the most well described PXR targets, *Cyp2c55* and *Cyp3a11* were further confirmed using RT-qPCR (Figure 2B). Interestingly, the "lipid metabolism" pathway was also highly significantly enriched upon PXR activation and, among the 30 genes with the highest fold-change, the patatin-like phospholipase domain containing 3 (*Pnpla3*), the thyroid hormone-responsive spot 14 (*Thrsp* or *Spot14*), and the growth/differentiation factor 15 (*Gdf15*) belonged to this pathway. Induction of *Gdf15* was also confirmed by RT-qPCR (Figure 2B).

We next investigated the effect of PCN on gene down-regulation. PCN treatment significantly decreased the expression of 186 genes in a PXR-dependent manner (Figure 2F). GO analyses revealed that these genes were involved in lipid metabolic process, biological rhythms, transforming growth factor-β (TGFβ) signaling pathway, glucose metabolism and cytochromes P450 (Figure 2G). The 30 genes with the highest fold-changes are illustrated in Figure 2H. Interestingly, among these 30 genes, 5 (namely *Fgf21*, *Cyp4a10*, *Cyp4a31*, *Acot1* and *Plin4*) are well-described target genes of PPARα, a key hepatic transcriptional regulator involved in lipid homeostasis.

Preprints (www.preprints.org) | NOT PEER-REVIEWED | Posted: 3 July 2019 doi:10.20944/preprints201907.0069.v1

Peer-reviewed version available at Int. J. Mol. Sci. 2019, 20, 3767; doi:10.3390/ijms20153767

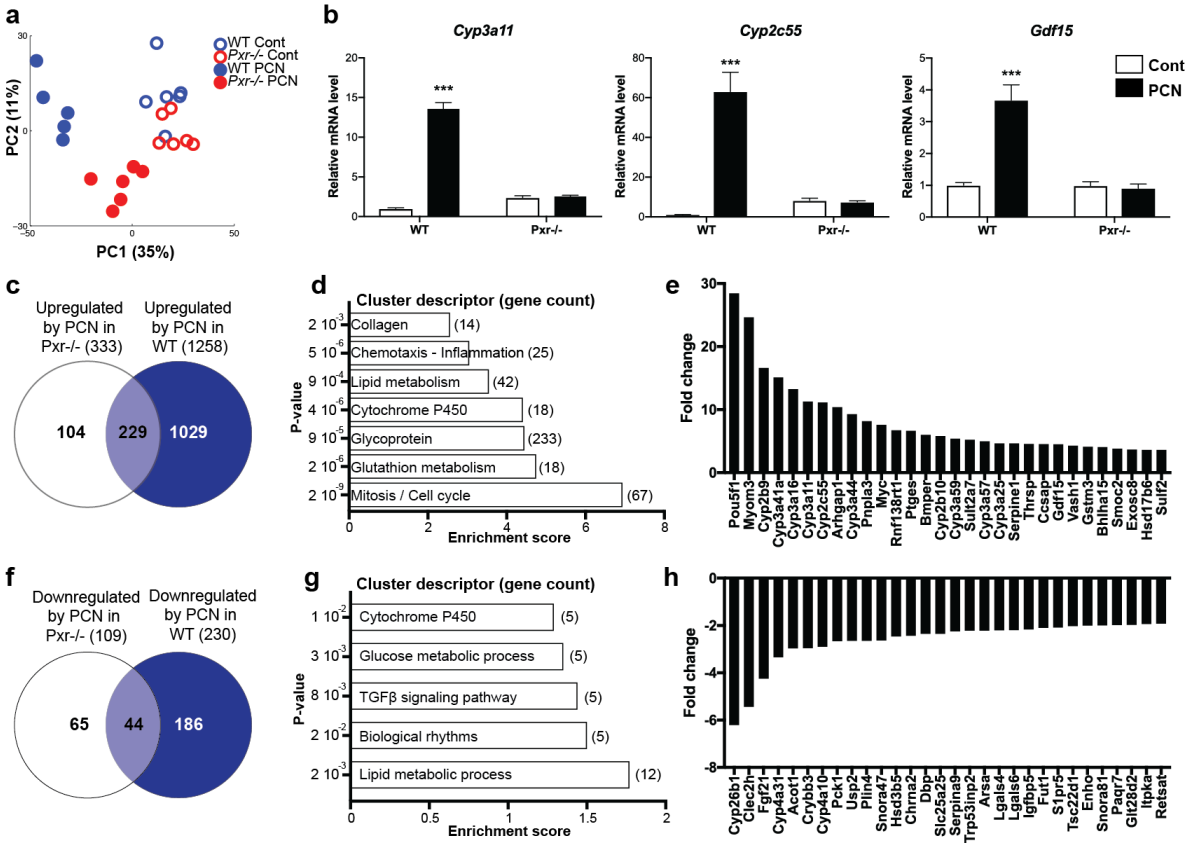

Figure 2. Impact of Pxr activation on the hepatic transcriptome. (a) PCA score plots of the whole transcriptomic dataset. (b) qPCR confirmation on selected genes. (c&e) Venn diagram representing the number of genes affected by PCN treatment. (d&g) Gene Enrichment Analyses of the PXR-target genes. (e&h) The 30 genes with the highest fold-changes upon PCN treatment.

2.3 Comparison of PXR and PPARα-dependent transcriptome

This prompted us to investigate whether PXR activation influenced PPARα activity. We took advantage of our previously published microarray dataset [14], in which C57Bl6/J male mice carrying an hepatocyte-specific deletion of *Pparα* (*Pparα*$^{hep-/-}$) were fasted for 24h to induce Pparα activity and compared to their wild-type littermates (*Pparα*$^{hep-/-}$). We have indeed previously shown that, during fasting, PPARα senses increased levels of free fatty acids released from adipocytes, and in response, controls the expression of hundreds of genes involved in fatty acid uptake, transport, and catabolism in hepatocytes [14,15]. Figure 3A indeed illustrates that a large number of the fasting-induced hepatic genes are PPARα sensitive, with 538 genes significantly up-regulated in a PPARα-dependent manner. Also, 461 genes were significantly down-regulated in a PPARα-dependant manner upon fasting (Figure 3D). We compared these genes with those regulated upon PXR activation. We found 27 genes that were both up-regulated upon PPARα activation and down-regulated upon PXR activation (Figure 3B). These genes are illustrated in Figure 3C and include, among others, *Pparα* itself, *Cyp4a14*, *Cyp4a10*, *Cyp4a31* and *Fgf21*. There were also 46 genes that were regulated in the opposite direction, i.e. that were downregulated upon PPARα activation and upregulated upon PXR activation (Figure 3E&F).

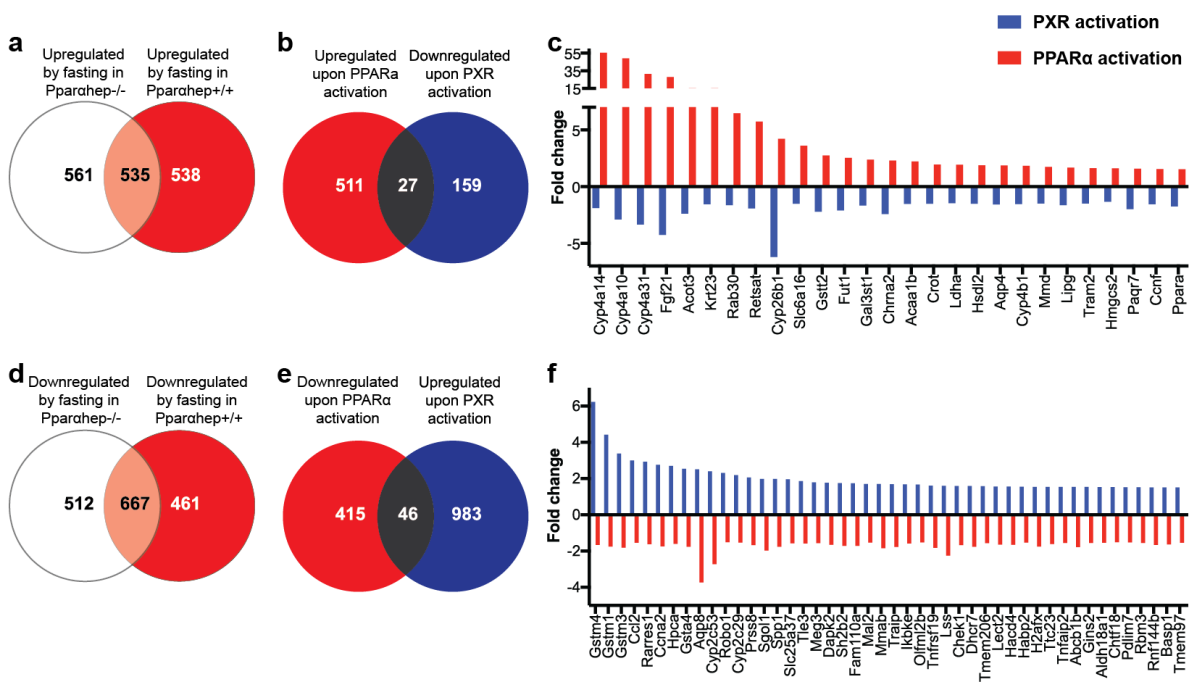

Figure 3. Comparison between PXR and PPARα target genes. (a&d) Venn diagrams representing the number of genes up- (a) or down- (d) regulated upon fasting in Pparα$^{hep+/+}$ vs. Pparα$^{hep-/-}$ mice. (b&e) Venn diagrams representing the number of genes regulated upon PPARα (red) or PXR (blue) activation. (c&f) Fold-changes for the genes that are shared in the previous Venn diagrams.

2.4 Regulation of FGF21

Using RT-qPCR analyses, we confirmed that PXR activation down-regulated *Pparα* and its target genes expression (Figure 4A), among which *Fgf21*. FGF21 is a recently described hepatokine with systemic metabolic effects [16]. We measured plasmatic FGF21 and confirmed that circulating FGF21 was decreased upon PCN treatment, since its levels were not detectable anymore in WT-treated mice (Figure 4B). Surprisingly, PXR deletion also influenced FGF21 level since *Pxr*$^{-/-}$ mice also showed no detectable levels of circulating FGF21.

Preprints (www.preprints.org) | NOT PEER-REVIEWED | Posted: 3 July 2019 doi:10.20944/preprints201907.0069.v1

Peer-reviewed version available at Int. J. Mol. Sci. 2019, 20, 3767; doi:10.3390/ijms20153767

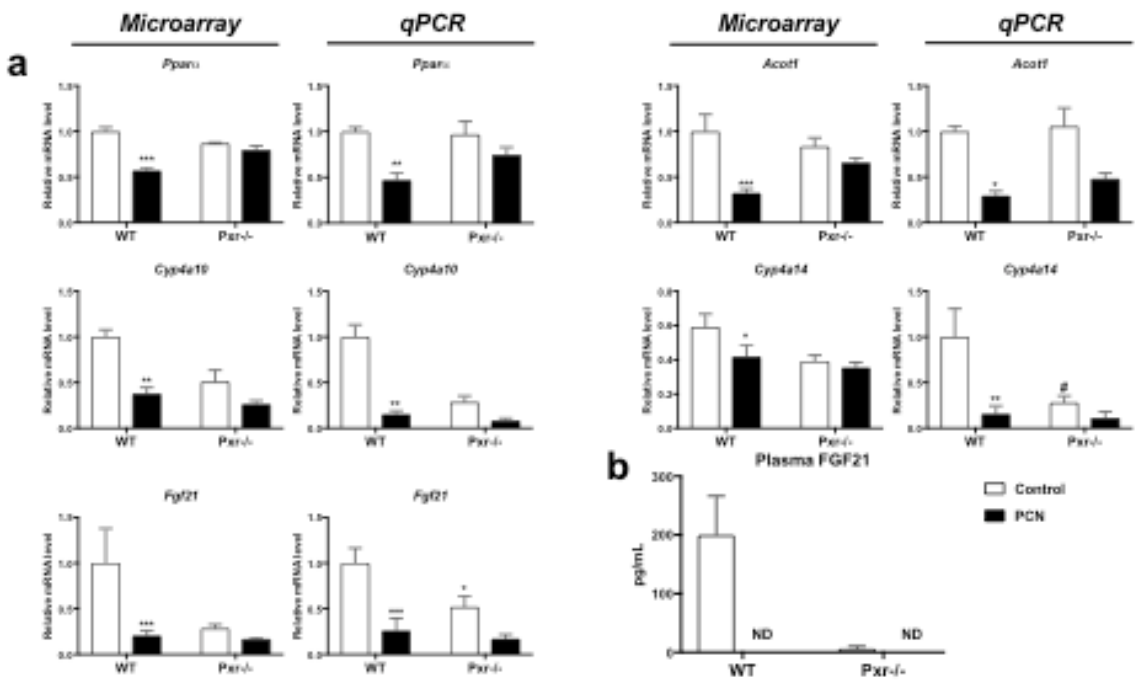

Figure 4. Impact of PXR activation on hepatic PPARα activity. Gene expression in the liver (a) derived from the microarray and from complementary qPCR experiments. (b) Plasma levels of FGF21. Data are mean±SEM of n=5-6 per group. *p≤0.05, **p≤0.01, ***p≤0.005 for PCN effect, #p≤0.05 for genotype effect using 2-way ANOVA and Tukey's post-tests. ND: not determined (under the limit of detection).

3. Discussion

The liver is one of the major organs involved in energy production. Hepatic lipid metabolism plays a crucial role during fasting and/or prolonged exercise. Upon lowering of blood glucose, the liver increases glucose production by augmenting gluconeogenesis and glycogenolysis to maintain blood glucose levels; increases fatty acid oxidation and ketogenesis to provide extra-hepatic tissues with ketone bodies; and decreases lipogenesis to attenuate triglyceride storage. These processes are under tight transcriptional control and, in response to hormones such as glucagon and glucocorticoids, many transcription factors cooperate to regulate various genes involved in metabolic pathways aimed at restoring homeostasis [17]. Among those, hepatic PPARα has been well described as crucial for this adaptation. However, recent data have highlighted that other nuclear receptors, such as the aryl H receptor (AhR), the constitutive androstane receptor (CAR) and PXR, which were historically described as xenobiotic sensors, can also interact with the hormone-responsive transcription factors to regulate the liver metabolic processes [18].

Here, we investigated the transcriptomic effects of a pharmacological activation of PXR. The expression of PXR was not described as highly circadian, however, its activity, as measured by the expression of its prototypical target gene *Cyp3a11*, has been shown to be influenced by the time of the day, and is highest as ZT6 [19].

Therefore, we decided to investigate the effects of PXR activation at ZT6, a time at which mice were in a physiological semi-fasted state.

Several studies have already investigated the hepatic signature of PXR activation *in vivo* [20-22] or *in vitro* [23]. However, most of these studies focused on the effect of PXR activation on xenobiotic metabolizing enzymes. Here, we confirm that regulation of xenobiotic metabolism is one of PXR's most potent functions in the hepatocytes (Figure 2; Supplementary Table 3). However, our gene enrichment analyses also revealed that lipid metabolism was among the top-dysregulated pathways upon PXR activation, considering both the up-regulated, as well as the down-regulated genes. Among the up-regulated genes, we observed that PXR activation increased the expression of several genes that correlates with lipogenesis such as the patatin-like phospholipase domain containing 3 (*Pnpla3*) and the thyroid hormone-responsive spot 14 (*Thrsp* or *Spot14*). Spot14 was first identified as a thyroid-responsive gene and is known to transduce hormone- and nutrient-related signals to genes involved in lipogenesis [24]. Regulation of SPOT14 by PXR was previously described in human hepatocytes [25] and led to increased fatty acid synthase (FASN) expression and triglyceride accumulation. The PNPLA3 protein has lipase activity towards triglycerides in hepatocytes and a loss-of-function polymorphism of this gene has been shown to be strongly associated with nonalcoholic fatty liver disease [26]. However, to our knowledge, the regulation of *Pnpla3* expression by PXR has not been previously described. Among the lipid-metabolic-related genes, we also observed that the expression of the growth/differentiation factor 15 (*Gdf15*), also known as MIC-1, was increased by a factor of 4 upon PCN treatment, in a PXR-dependent way. GDF15 is a distant member of the transforming growth factor-ß (TGF-ß) superfamily that is considered as a crucial hormone in regulating lipid and carbohydrate metabolism. In animal models, overexpression of GDF15 leads to a lean phenotype and improvements of metabolic parameters by increasing the expression of key thermogenic and lipolytic genes in brown and white adipose tissue [27]. Hepatic and circulating GDF15 levels were also increased in animals with blunted ß-oxidation (*Cpt2*$^{hep-/-}$ mice) to maintain systemic energy homeostasis upon fasting [28]. Whether the observed increase in *Gdf15* mRNA upon PCN treatment results from a direct regulation of *Gdf15* by PXR or represents a secondary adaptation to decreased ß-oxidation remains to be determined. In both cases, regulation of GDF15 levels upon PXR activation might be of physiological relevance since GDF15 has been implicated in a wide variety of biological functions including control of food intake and body weight [29].

Among the genes that were down-regulated upon PXR activation, we observed a very consistent PPARα-like signature, with the decreased expression of many *Cyp4* genes, which are highly sensitive PPARα target genes [14,15]. These results coincide with previous findings in which PCN decreased the hepatic expression of *Pparα*, *Cyp4a10* and *Cyp4a14* [21]. Neonatal exposure to a single dose of PCN also persistently down-regulated Cyp4a expression and decreased PPARα binding to

the Cyp4a gene loci in adult mice [20]. By comparing the list of genes down-regulated upon PXR activation to a list a genes up-regulated upon PPARα activation, we here extend these previous findings and demonstrate that the inhibition of PPARα activity by PXR affects more than the expression of Cyp4 genes. For example, the PXR-PPARα interaction probably inhibited the expression of the acetyl-Coenzyme A acyltransferase 1B (*Acaa1b*), of the acyl-coA thioeserase 3 (*Acot3*), of *Krt23* and *Rab30*, of the rate limiting enzyme in ketogenesis 3-hydroxy-3-methylglutaryl-CoenzymeA synthase 2 (*Hmgcs2*) and of the hepatokine *Fgf21*, all of which are well-described PPARα targets [14]. Using a similar approach in human primary hepatocytes treated with the hPXR ligand rifampicine and the hPPARα ligand WY14643, Kandel et al. had previously shown that more than 14 genes were responsive to both WY14643 (up-regulated) and to rifampicine (down-regulated), among which ACAA2, CYP4A11 and HMGCS2 [23], therefore suggesting the human relevance of our results.

FGF21 is predominantly produced in the liver [30] and exerts pleiotropic effects on the body to maintain overall metabolic homeostasis. FGF21 metabolic benefits range from reducing body weight to alleviating hyperglycaemia and insulin resistance and improvement of lipid profiles [16]. Although PXR is mainly expressed in the liver and in the intestine, and not in adipose tissue [31], deletion of *Pxr* appear to influence insulin sensitivity also in white adipose tissue and in the muscle [32], serum leptin and adiponectin levels [33] and PXR activation regulates gene expression in both white and brown adipose tissues [34]. This suggests systemic effects of *Pxr* deletion and activation for which mechanisms have not been described yet. White and brown adipose tissues are among the most described target tissues of FGF21 [16]. Whether FGF21 could be an effector of the systemic effects of PXR remains an open question. Here, we demonstrate that both PXR-activation and PXR deletion decrease the hepatic *Fgf21* mRNA levels and completely abolished the circulating FGF21 levels.

Perspectives and limitations of our study include the use of male mice only, while PXR activation has been shown to impact both xenobiotic metabolizing exzymes and glucose and lipid metabolism in a sexually-dimorphic way [35,36]. Therefore, it would be interesting to decipher whether the signature of PXR activation described in our study is also valid in female mice. Second, our study focused on short-term changes. An important remaining question is to determine the effect of multiple weak PXR agonists such as those present in our environment on the observed regulations, especially on FGF21 secretion.

Altogether, our results present an additional resource of transcriptome analyses that confirm and extend previous findings on the genes involved in the pro-steatotic effects of PXR. As previously observed in various models [7], we confirm that the observed pro-steatotic effect of PXR activation probably results from both induction of lipogenesis and repression of β-oxidation, and further

Peer-reviewed version available at Int. J. Mol. Sci. 2019, 20, 3767; doi:10.3390/ijms20153767

highlight that this repression is certainly mediated, as least in part, through inhibition of PPARα. We also provide new hypotheses regarding the yet poorly explored pleiotropic effects of PXR that could result from regulation of recently discovered hepatokines such as GDF15 and/or FGF21. More studies are needed to confirm the physiological relevance of these regulations. Our findings might have clinical and public health relevance given the wide range of drugs and environmental xenobiotics that have been described as PXR ligands and potential endocrine disruptors.

4. Materials and Methods

Animals

In vivo studies were performed in a conventional laboratory animal room following the European Union guidelines for laboratory animal use and care. The current project was approved by an independent ethics committee (CEEA-86 Toxcométhique) under the authorization number 2018062810452910). The animals were treated humanely with due consideration to the alleviation of distress and discomfort. All mice were housed at 21-23°C on a 12-hour light (ZT0-ZT12) 12-hour dark (ZT12-ZT24) cycle and allowed free access to the diet (Teklad Global 18% Protein Rodent Diet) and tap water. ZT stands for Zeitgeber time; ZT0 is defined as the time when the lights are turned on. Twelve six-week old wild-type (WT) C57BL/6J male mice were purchased from Charles River and 12 *Pxr*$^{-/-}$ animals (backcrossed on the C57Bl/6J background) were engineered in Pr. Meyer's laboratory [37] and are bred for 10y in our animal facility. Mice were acclimatized for two weeks, then randomly allocated to the different experimental groups: wild-type control (WT CONT, n=6), wild-type PCN-treated (WT PCN, n=6), *Pxr*$^{-/-}$ control (*Pxr*$^{-/-}$ CONT, n=6), *Pxr*$^{-/-}$ PCN-treated (*Pxr*$^{-/-}$ PCN, n=6). PCN-treated mice received a daily intraperitoneal injection of PCN (100 mg/kg) in corn oil for 4 days while control mice received corn oil only. Mice were killed at ZT6, 6 hours after the last PCN injection.

Blood and tissue samples

Body weight was monitored at the beginning and at the end of experimental period. Prior to sacrifice, the submandibular vein was lanced, and blood was collected into lithium heparin-coated tubes (BD Microtainer). Plasma was prepared by centrifugation (1500 g, 10 min, 4°C) and stored at -80°C. At sacrifice, the liver, the three parts of the small intestine (duodenum, jejunum, ileum), and the colon were removed and snap-frozen in liquid nitrogen and stored at -80°C until used for RNA extraction.

Gene expression

Peer-reviewed version available at Int. J. Mol. Sci. 2019, 20, 3767; doi:10.3390/ijms20153767

Total RNA was extracted with TRIzol reagent (Invitrogen). Gene expression profiles were obtained at the GeT-TRiX facility (GénoToul, Génopole Toulouse Midi-Pyrénées, France) using Sureprint G3 Mouse GE v2 microarrays (8x60K; design 074,809; Agilent technologies) following the manufacturer's instructions Microarray data and experimental details are available in NCBI's Gene Expression Omnibus [38] and are accessible through GEO Series accession numbers GSE123804. For real-time quantitative polymerase chain reaction (qPCR), 2 µg RNA samples were reverse-transcribed using the High-Capacity cDNA Reverse Transcription Kit (Applied Biosystems). Supplementary Table 1 presents the SYBR Green assay primers. Amplifications were performed using an ABI Prism 7300 Real-Time PCR System (Applied Biosystems). qPCR data were normalised to TATA-box-binding protein mRNA levels, and analyzed with LinRegPCR.v2015.3.

Plasma analysis

Alanine transaminase (ALT), total cholesterol, triglycerides and free fatty acids (FFA) were determined using a Pentra 400 biochemical analyzer (Anexplo facility, Toulouse, France). Plasma FGF21 was assayed using the rat/mouse FGF21 ELISA kit (EMD Millipore) following the manufacturer's instructions.

Liver neutral lipid analysis

Tissue samples were homogenized in methanol/5 mM EGTA (2:1, v/v); then, lipids (corresponding to an equivalent of 2 mg tissue) were extracted according to the Bligh and Dyer method [39] with chloroform/methanol/water (2.5:2.5:2.1, v/ v/v), in the presence of the following internal standards: glyceryl trinonadecanoate, stigmasterol, and cholesteryl heptadecanoate (Sigma). Triglycerides, free cholesterol, and cholesterol esters were analysed with gas-liquid chromatography on a Focus Thermo Electron system equipped with a Zebron-1 Phenomenex fused-silica capillary column (5 m, 0.25 mm i.d., 0.25 mm film thickness). Oven temperature was programmed to increase from 200 to 350° C at 5 °C/min, and the carrier gas was hydrogen (0.5 bar). Injector and detector temperatures were 315 °C and 345 °C respectively.

Statistical analysis

Microarray data were processed using R (http://www.r-project.org) and Bioconductor packages (www.bioconductor.org, v 3.0, Gentleman, Carey et al. 2004). Raw data (median signal intensity) were filtered, log2 transformed, corrected for batch effects (microarray washing bath) and normalized using CrossNorm method [40]. Normalized data were first analysed using Matlab (v2014.8). Principal component analysis was performed using an in-house function. Linear model was fitted using the limma lmFit function [41]. Pair-wise comparisons between biological conditions were applied using specific contrasts. A correction for multiple testing was applied using Benjamini-Hochberg procedure for False

Peer-reviewed version available at Int. J. Mol. Sci. 2019, 20, 3767; doi:10.3390/ijms20153767

Discovery Rate (FDR). Probes with FDR ≤ 0.05 and |fold-change| > 1.5 were considered to be differentially expressed between conditions. Gene-annotation enrichment analysis and functional annotation clustering were evaluated using DAVID [42]. For non- microarray data, differential effects were analyzed by analysis of variance followed by Tukey's post-hoc tests. A p-value <0.05 was considered significant.

Author Contributions: Conceptualization, H.G and S.E.S.; methodology, S.A.B, F.L.A, S.S, C.L, T.F.; software, Y.L.; formal analysis, S.A.B, Y.L. and S.E.S. ; investigation, S.A.B, F.L. M.R., A.P. writing—original draft preparation, S.A.B, S.E.S.; writing—review and editing, A.F., C.L., H.G and S.E.S.; supervision, H.G, L.G.P, L.M.L, N.L and S.E.S.; project administration, H.G, L.G.P, L.M.L, N.L and S.E.S.; funding acquisition, H.G, L.G.P, L.M.L, N.L and S.E.S.

Funding: S.A.B. is supported by a PhD grant from Région Occitanie and INRA AlimH department. This work was supported by grants from Agence Nationale de la Recherche (ANR), Fond Européen de Développement Régional (FEDER) and Région Occitanie. SES is supported by a Joint Programming Initiative (JPI) grant Fatmal.

Acknowledgments: We thank all members of the EZOP staff for their careful help with this project. We thank the staff from the Genotoul: Anexplo, Get-TriX and Metatoul-Lipidomic facilities. Pxr-/- mice are a generous gift from Pr Steven Kliewer (University of Texas Southwestern Medical School, Dallas, TX, USA). Colony founders were kindly provided by Pr Urs A Meyer (Biozentrum, University of Basel, Basel, Switzerland).

Conflicts of Interest: "The authors declare no conflict of interest."

Abbreviations

ACAA	acetyl-Coenzyme A acyltransferase
Acot	acyl-coA thioeserase
AhR	aryl H receptor
CAR	cytochrome P450
Cpt	carnitine palmitoyltransferase
CYP	constitutive androstane receptor
DR4	direct repeat 4
FASN	fatty acid synthase
FDR	false discovery rate
FGF21	fibroblast growth factor 21
G6Pase	glucose-6-phosphatase
GDF15	growth/differentiation factor 15
GCK	glucokinase
GO	gene ontology
GLUT2	glucose transporter 2
HMGCS	3-hydroxy-3-methylglutaryl-CoenzymeA synthase
hPPARα	Human PPARα
hPXR	human PXR
Krt23	keratin 23
PXR	pregnane X receptor
PXRE	pregnane X receptor response elements
PCA	principal component analysis

Peer-reviewed version available at Int. J. Mol. Sci. 2019, 20, 3767; doi:10.3390/ijms20153767

PCN	pregnenolone 16α-carbonitrile
PEPCK	phosphoenopyruvate carboxykinase
PNPLA3	patatin-like phospholipase domain containing 3
PPARα	peroxisome proliferator-activated receptor α
Rab30	ras-related protein rab-30
RT-qPCR	quantitative reverse transcription PCR
RXR	retinoid X receptor
SPOT14	thyroid hormone-responsive spot 14
TGFβ	transforming growth factor-ß
Thrsp	thyroid hormone-responsive spot 14
WT	wild-type
ZT	Zeitgeber time

References

1. Bookout, A. L.; Jeong, Y.; Downes, M.; Yu, R. T.; Evans, R. M.; Mangelsdorf, D. J. Anatomical profiling of nuclear receptor expression reveals a hierarchical transcriptional network. *Cell* **2006**, *126*, 789–799.

2. Kliewer, S. A.; Moore, J. T.; Wade, L.; Staudinger, J. L.; Watson, M. A.; Jones, S. A.; McKee, D. D.; Oliver, B. B.; Willson, T. M.; Zetterström, R. H.; Perlmann, T.; Lehmann, J. M. An orphan nuclear receptor activated by pregnanes defines a novel steroid signaling pathway. *Cell* **1998**, *92*, 73–82.

3. Hernandez, J. P.; Mota, L. C.; Baldwin, W. S. Activation of CAR and PXR by Dietary, Environmental and Occupational Chemicals Alters Drug Metabolism, Intermediary Metabolism, and Cell Proliferation. *Curr Pharmacogenomics Person Med* **2009**, *7*, 81–105.

4. Guengerich, F. P. Cytochrome P-450 3A4: regulation and role in drug metabolism. *Annu Rev Pharmacol Toxicol* **1999**, *39*, 1–17.

5. Drozdzik, M.; Busch, D.; Lapczuk, J.; Müller, J.; Ostrowski, M.; Kurzawski, M.; Oswald, S. Protein Abundance of Clinically Relevant Drug-Metabolizing Enzymes in the Human Liver and Intestine: A Comparative Analysis in Paired Tissue Specimens. *Clinical Pharmacology & Therapeutics* **2018**, *104*, 515–524.

6. Yu, J.; Petrie, I. D.; Levy, R. H.; Ragueneau-Majlessi, I. Mechanisms and Clinical Significance of Pharmacokinetic-based Drug-drug Interactions with Drugs Approved by the U.S. Food and Drug Administration in 2017. *Drug Metab. Dispos.* **2018**, dmd.118.084905.

7. Hakkola, J.; Rysä, J.; Hukkanen, J. Regulation of hepatic energy metabolism by the nuclear receptor PXR. *Biochim Biophys Acta* **2016**.

8. Kodama, S.; Koike, C.; Negishi, M.; Yamamoto, Y. Nuclear receptors CAR and PXR cross talk with FOXO1 to regulate genes that encode drug-metabolizing and gluconeogenic enzymes. *Mol. Cell. Biol.* **2004**, *24*, 7931–7940.

9. Rysä, J.; Buler, M.; Savolainen, M. J.; Ruskoaho, H.; Hakkola, J.; Hukkanen, J. Pregnane X receptor agonists impair postprandial glucose tolerance. *Clinical Pharmacology & Therapeutics* **2013**, *93*, 556–563.

10. Bitter, A.; Rümmele, P.; Klein, K.; Kandel, B. A.; Rieger, J. K.; Nüssler, A. K.; Zanger, U. M.; Trauner, M.; Schwab, M.; Burk, O. Pregnane X receptor activation and silencing promote steatosis of human hepatic cells by distinct lipogenic mechanisms. *Arch. Toxicol.* **2015**, *89*, 2089–2103.

11. Meng, Z.; Gwag, T.; Sui, Y.; Park, S.-H.; Zhou, X.; Zhou, C. The atypical antipsychotic quetiapine induces hyperlipidemia by activating intestinal PXR signaling. *JCI Insight* **2019**, *4*, 1.

12. Gwag, T.; Meng, Z.; Sui, Y.; Helsley, R. N.; Park, S.-H.; Wang, S.; Greenberg, R. N.; Zhou, C. Non-nucleoside reverse transcriptase inhibitor efavirenz activates PXR to induce hypercholesterolemia and hepatic steatosis. *J Hepatol* **2019**, *70*, 930–940.

13. Kliewer, S. A.; Mangelsdorf, D. J. A Dozen Years of Discovery: Insights into the Physiology and Pharmacology of FGF21. *Cell Metab* **2019**, *29*, 246–253.

14. Régnier, M.; Polizzi, A.; Lippi, Y.; Fouché, E.; Michel, G.; Lukowicz, C.; Smati, S.; Marrot, A.; Lasserre, F.; Naylies, C.; Batut, A.; Viars, F.; Bertrand-Michel, J.; Postic, C.; Loiseau, N.; Wahli, W.; Guillou, H.; Montagner, A. Insights into the role of hepatocyte PPARα activity in response to fasting. *Mol. Cell. Endocrinol.* **2017**.

15. Montagner, A.; Polizzi, A.; Fouché, E.; Ducheix, S.; Lippi, Y.; Lasserre, F.; Barquissau, V.; Régnier, M.; Lukowicz, C.; Benhamed, F.; Iroz, A.; Bertrand-Michel, J.; Saati, Al, T.; Cano, P.; Mselli-Lakhal, L.; Mithieux, G.; Rajas, F.; Lagarrigue, S.; Pineau, T.; Loiseau, N.; Postic, C.; Langin, D.; Wahli, W.; Guillou, H. Liver PPARα is crucial for whole-body fatty acid homeostasis and is protective against NAFLD. *Gut* **2016**, *65*, 1202–1214.

16. BonDurant, L. D.; Potthoff, M. J. Fibroblast Growth Factor 21: A Versatile Regulator of Metabolic Homeostasis. *Annual Review of Nutrition* **2018**, *38*, 173–196.

17. Goldstein, I.; Hager, G. L. Transcriptional and Chromatin Regulation during Fasting – The Genomic Era. *Trends in Endocrinology & Metabolism* **2015**, *26*, 699–710.

18. Konno, Y.; Negishi, M.; Kodama, S. The roles of nuclear receptors CAR and PXR in hepatic energy metabolism. *Drug Metab. Pharmacokinet.* **2008**, *23*, 8–13.

19. Montagner, A.; Korecka, A.; Polizzi, A.; Lippi, Y.; Blum, Y.; Canlet, C.; Tremblay-Franco, M.; Gautier-Stein, A.; Burcelin, R.; Yen, Y.-C.; Je, H. S.; Maha, A.-A.; Mithieux, G.; Arulampalam, V.; Lagarrigue, S.; Guillou, H.; Pettersson, S.; Wahli, W. Hepatic circadian clock oscillators and nuclear receptors integrate microbiome-derived signals. *Sci Rep* **2016**, *6*, 20127.

20. Li, C. Y.; Cheng, S. L.; Bammler, T. K.; Cui, J. Y. Editor's Highlight: Neonatal Activation of the Xenobiotic-Sensors PXR and CAR Results in Acute and Persistent Down-regulation of PPARα-Signaling in Mouse Liver. *Toxicol Sci* **2016**, *153*, 282–302.

21. Cui, J. Y.; Klaassen, C. D. RNA-Seq reveals common and unique PXR- and CAR-target gene signatures in the mouse liver transcriptome. *Biochim Biophys Acta* **2016**.

22. Nagahori, H.; Nakamura, K.; Sumida, K.; Ito, S.; Ohtsuki, S. Combining Genomics To Identify the Pathways of Post-Transcriptional Nongenotoxic Signaling and Energy Homeostasis in Livers of Rats Treated with the Pregnane X Receptor Agonist, Pregnenolone Carbonitrile. *Journal of proteome research* **2017**, *16*, 3634–3645.

23. Kandel, B. A.; Thomas, M.; Winter, S.; Damm, G.; Seehofer, D.; Burk, O.; Schwab, M.; Zanger, U. M. Genomewide comparison of the inducible transcriptomes of nuclear receptors CAR, PXR and PPARα in primary human hepatocytes. *Biochim Biophys Acta* **2016**.

24. LaFave, L. T.; Augustin, L. B.; Mariash, C. N. S14: insights from knockout mice. *Endocrinology* **2006**, *147*, 4044–4047.

25. Moreau, A.; Téruel, C.; Beylot, M.; Albalea, V.; Tamasi, V.; Umbdenstock, T.; Parmentier, Y.; Sa-Cunha, A.; Suc, B.; Fabre, J.-M.; Navarro, F.; Ramos, J.; Meyer, U.; Maurel, P.; Vilarem, M.-J.; Pascussi, J. M. A novel pregnane X receptor and S14-mediated lipogenic pathway in human hepatocyte. *Hepatology* **2009**, *49*, 2068–2079.

26. Dai, G.; Liu, P.; Li, X.; Zhou, X.; He, S. Association between PNPLA3 rs738409 polymorphism and nonalcoholic fatty liver disease (NAFLD) susceptibility and severity: A meta-analysis. *Medicine (Baltimore)* **2019**, *98*, e14324.

27. Chrysovergis, K.; Wang, X.; Kosak, J.; Lee, S.-H.; Kim, J. S.; Foley, J. F.; Travlos, G.; Singh, S.; Baek, S. J.; Eling, T. E. NAG-1/GDF-15 prevents obesity by increasing thermogenesis, lipolysis and oxidative metabolism. *Int J*

463 *Obes (Lond)* **2014**, *38*, 1555–1564.
464 28. Lee, J.; Choi, J.; Scafidi, S.; Wolfgang, M. J. Hepatic Fatty Acid Oxidation Restrains Systemic Catabolism
465 during Starvation. *Cell Rep* **2016**, *16*, 201–212.
466 29. Mullican, S. E.; Lin-Schmidt, X.; Chin, C.-N.; Chavez, J. A.; Furman, J. L.; Armstrong, A. A.; Beck, S. C.;
467 South, V. J.; Dinh, T. Q.; Cash-Mason, T. D.; Cavanaugh, C. R.; Nelson, S.; Huang, C.; Hunter, M. J.; Rangwala, S.
468 M. GFRAL is the receptor for GDF15 and the ligand promotes weight loss in mice and nonhuman primates. *Nat*
469 *Med* **2017**, *23*, 1150–1157.
470 30. Markan, K. R.; Naber, M. C.; Ameka, M. K.; Anderegg, M. D.; Mangelsdorf, D. J.; Kliewer, S. A.;
471 Mohammadi, M.; Potthoff, M. J. Circulating FGF21 is liver derived and enhances glucose uptake during
472 refeeding and overfeeding. *Diabetes* **2014**, *63*, 4057–4063.
473 31. Ellero-Simatos, S.; Chakhtoura, G.; Barreau, C.; Langouët, S.; Benelli, C.; Penicaud, L.; Beaune, P.; de
474 Waziers, I. Xenobiotic-metabolizing cytochromes p450 in human white adipose tissue: expression and
475 induction. *Drug Metab. Dispos.* **2010**, *38*, 679–686.
476 32. He, J.; Gao, J.; Xu, M.; Ren, S.; Stefanovic-Racic, M.; O'Doherty, R. M.; Xie, W. PXR ablation alleviates
477 diet-induced and genetic obesity and insulin resistance in mice. *Diabetes* **2013**, *62*, 1876–1887.
478 33. Spruiell, K.; Richardson, R. M.; Cullen, J. M.; Awumey, E. M.; Gonzalez, F. J.; Gyamfi, M. A. Role of pregnane
479 X receptor in obesity and glucose homeostasis in male mice. *The Journal of Biological Chemistry* **2014**, *289*,
480 3244–3261.
481 34. Ma, Y.; Liu, D. Activation of pregnane X receptor by pregnenolone 16 α-carbonitrile prevents high-fat
482 diet-induced obesity in AKR/J mice. *PLoS ONE* **2012**, *7*, e38734.
483 35. Lu, Y.-F.; Jin, T.; Xu, Y.; Zhang, D.; Wu, Q.; Zhang, Y.-K. J.; Liu, J. Sex differences in the circadian variation of
484 cytochrome p450 genes and corresponding nuclear receptors in mouse liver. *Chronobiol. Int.* **2013**, *30*, 1135–1143.
485 36. Spruiell, K.; Gyamfi, A. A.; Yeyeodu, S. T.; Richardson, R. M.; Gonzalez, F. J.; Gyamfi, M. A. Pregnane X
486 Receptor-Humanized Mice Recapitulate Gender Differences in Ethanol Metabolism but Not Hepatotoxicity. *J*
487 *Pharmacol Exp Ther* **2015**, *354*, 459–470.
488 37. Staudinger, J. L.; Goodwin, B.; Jones, S. A.; Hawkins-Brown, D.; MacKenzie, K. I.; LaTour, A.; Liu, Y.;
489 Klaassen, C. D.; Brown, K. K.; Reinhard, J.; Willson, T. M.; Koller, B. H.; Kliewer, S. A. The nuclear receptor PXR
490 is a lithocholic acid sensor that protects against liver toxicity. *Proc Natl Acad Sci USA* **2001**, *98*, 3369–3374.
491 38. Edgar, R.; Domrachev, M.; Lash, A. E. Gene Expression Omnibus: NCBI gene expression and hybridization
492 array data repository. *Nucleic Acids Res* **2002**, *30*, 207–210.
493 39. Bligh, E. G.; Dyer, W. J. A RAPID METHOD OF TOTAL LIPID EXTRACTION AND PURIFICATION.
494 *Canadian Journal of Biochemistry and Physiology* **2011**, *37*, 911–917.
495 40. Cheng, L.; Lo, L.-Y.; Tang, N. L. S.; Wang, D.; Leung, K.-S. CrossNorm: a novel normalization strategy for
496 microarray data in cancers. *Sci Rep* **2016**, *6*, 18898.
497 41. Smyth, G. K. Linear models and empirical bayes methods for assessing differential expression in microarray
498 experiments. *Stat Appl Genet Mol Biol* **2004**, *3*, Article3–25.
499 42. Huang, D. W.; Sherman, B. T.; Lempicki, R. A. Bioinformatics enrichment tools: paths toward the
500 comprehensive functional analysis of large gene lists. *Nucleic Acids Res* **2009**, *37*, 1–13.
501